ARTICLE

ST6GAL1 inhibits metastasis of hepatocellular carcinoma via modulating sialylation of MCAM on cell surface

Xia Zou[1,2,7], Jishun Lu[1,7], Yao Deng[1,7], Qiannan Liu[1], Xialin Yan[3], Yalu Cui[1], Xiao Xiao[4], Meng Fang[5], Fang Yang[1], Hiromichi Sawaki[6], Takashi Sato[2,6], Binbin Tan[1,2], Xiaoyan Lu[1], Bo Feng[3], Atsushi Kuno[2,6], Hisashi Narimatsu[2,6], Chunfang Gao[4] and Yan Zhang[1,2]✉

The poor prognosis of hepatocellular carcinoma (HCC) is mainly because of its high rate of metastasis. Thus, elucidation of the molecular mechanisms underlying HCC metastasis is of great significance. Glycosylation is an important post-translational modification that is closely associated with tumor progression. Altered glycosylation including the altered sialylation resulting from aberrant expression of β-galactoside α2,6 sialyltransferase 1 (ST6GAL1) has long been considered as an important feature of cancer cells. However, there is limited information on the roles of ST6GAL1 and α2,6 sialylation in HCC metastasis. Here, we found that ST6GAL1 and α2,6 sialylation were negatively correlated with the metastatic potentials of HCC cells. Moreover, ST6GAL1 overexpression inhibited migration and invasion of HCC cells in vitro and suppressed HCC metastasis in vivo. Using a metabolic labeling-based glycoproteomic strategy, we identified a list of sialylated proteins that may be regulated by ST6GAL1. In particular, an increase in α2,6 sialylation of melanoma cell adhesion molecule (MCAM) inhibited its interaction with galectin-3 and decreased its expression on cell surface. In vitro and in vivo analysis showed that ST6GAL1 exerted its function in HCC metastasis by regulating MCAM expression. Finally, we found the relative intensity of sialylated MCAM was negatively correlated with tumor malignancy in HCC patients. Taken together, these results demonstrate that ST6GAL1 may be an HCC metastasis suppressor by affecting sialylation of MCAM on cell surface, which provides a novel insight into the roles of ST6GAL1 in HCC progression and supports the functional complexity of ST6GAL1 in a cancer type- and tissue type-specific manner.

Oncogene; https://doi.org/10.1038/s41388-022-02571-9

INTRODUCTION

Hepatocellular carcinoma (HCC), the most common type of primary liver cancer, is among the leading causes of global cancer-related mortality. There are approximately 830,000 deaths due to HCC per year worldwide [1], of which ~50% occur in China [2]. Despite significant progress in HCC treatment, the overall prognosis of HCC patients remains poor with an average 5-year survival rate of 18% [3]. A main reason is the high rate of metastasis and recurrence of HCC [4]. Therefore, better understanding of the molecular mechanism underlying metastasis is critical to effectively intervene tumor development and improve the prognosis of HCC patients.

Glycosylation is one of the most common post-translational modifications of proteins, which is crucial for a wide variety of fundamental molecular and cellular processes [5]. Glycosylation alterations in cells are highly sensitive to the physiological state. When a normal cell transforms progressively to a neoplastic state, the glycan profile will be specifically altered because of various factors including dysregulation of glycosyltransferases and glycosidases [6, 7]. To date, the most widely occurring cancer-associated glycosylations include abnormal expression of sialylation, fucosylation, increased truncated O-glycans and branched N-glycans. Functionally, these structures are involved in crucial events in cancer, ranging from inflammation, angiogenesis, invasion and metastasis [6, 7]. Therefore, investigation of aberrant glycans on specific proteins regulated by glycosyltransferase is important to understand the mechanisms of tumor progression and metastasis, and develop new biomarkers for cancer diagnosis and treatment. In fact, some cancer-associated glycans/glycoproteins have been used in the clinic, such as carcinoembryonic antigen (CEA), mucin-16, and prostate-specific antigen (PSA) [8].

Sialylation is a terminal modification in cellular glycosylation, which plays important roles in cell-cell communication, cellular recognition, and cell adhesion, and affects circulating half-lives of many glycoproteins. Among the various sialylation forms, α2,6-linked sialic acid of N-glycans is a common and important pattern, which is primarily synthesized by β-galactoside α2,6 sialyltransferase 1 (ST6GAL1) in humans [9]. Aberrant

[1]Key Laboratory of Systems Biomedicine (Ministry of Education), Shanghai Center for Systems Biomedicine, Shanghai Jiao Tong University, Shanghai 200240, China. [2]SCSB (China)-AIST (Japan) Joint Medical Glycomics Laboratory, Shanghai Jiao Tong University, Shanghai 200240, China. [3]Department of General Surgery, Shanghai Minimally Invasive Surgery Center, Ruijin Hospital, Shanghai Jiao Tong University School of Medicine, Shanghai 200025, China. [4]Clinical Laboratory Medicine Center, Yueyang Hospital of Integrated Traditional Chinese and Western Medicine, Shanghai University of Traditional Chinese Medicine, Shanghai 200437, China. [5]Department of Laboratory Medicine, Shanghai Eastern Hepatobiliary Surgery Hospital, Shanghai 200438, China. [6]Molecular and Cellular Glycoproteomics Research Group, Cellular and Molecular Biotechnology Research Institute, National Institute of Advanced Industrial Science and Technology, Tsukuba, Ibaraki 305-8568, Japan. [7]These authors contributed equally: Xia Zou, Jishun Lu, Yao Deng. ✉email: yanzhang2006@sjtu.edu.cn

Received: 21 December 2021 Revised: 24 November 2022 Accepted: 7 December 2022
Published online: 17 December 2022

expression of α2,6 sialylation and ST6GAL1 are frequently observed in tumor cells and linked to patient prognosis [9, 10]. In particular, up-regulation of ST6GAL1 has been reported to induce a more invasive cell phenotype and promote tumor metastatic progression in pancreatic, ovarian, breast, cervical, colon, gastric cancer, etc. [11–16]. The mechanisms include integrin-mediated process, EGFR-mediated epithelial to mesenchymal transition (EMT), and death receptors-mediated apoptosis [11, 17, 18]. However, compared with these cancers, much less is known about the roles of ST6GAL1 and α2,6 sialylation in HCC metastasis so far.

In this study, we demonstrate that ST6GAL1 and α2,6 sialylation were negatively correlated with HCC metastasis. Overexpression of ST6GAL1 suppressed tumor migration and metastasis in vitro and in vivo. Using a metabolic labeling-based glycoproteomic strategy, we found that melanoma cell adhesion molecule (MCAM) was regulated by ST6GAL1, and its sialylation inhibited the interaction between MCAM and galectin-3 and suppressed the dimerization of MCAM on cell surface. Furthermore, we verified ST6GAL1 exerted its function in HCC metastasis by regulating MCAM expression, and the levels of sialylated MCAM was negatively correlated with tumor malignancy in HCC patients.

RESULTS

ST6GAL1 is negatively correlated with the metastatic potentials of HCC cell lines

To investigate the role of glycosylation in HCC metastasis, we first examined the glycosylation pattern of two HCC cell lines with similar genetic backgrounds, but different metastatic potentials (MHCC97L < HCCLM3) [19]. In contrast to the little/small difference in the reactivity of other lectins between these two cell lines, the lectin array analysis showed that three lectins, *Sambucus nigra* agglutinin (SNA), *Sambucus sieboldiana* agglutinin (SSA), and *Trichosanthes japonica* agglutinin-I (TJA-I), which primarily recognize α2,6 sialylation on N-glycans, exhibited markedly lower reactivities toward HCCLM3 compared with MHCC97L (Fig. 1A). The quantitative mRNA assay of 20 sialyltransferase transcription revealed that ST6GAL1, which mainly produces α2,6-linked sialic acids on N-glycans, was approximately 50-fold lower in HCCLM3 cells than in MHCC97L cells (Fig. 1B). These observations were confirmed by cell surface glycosylation assay and qRT-PCR of ST6GAL1 (Fig. 1C, D), suggesting that ST6GAL1 expression negatively correlates with the metastatic ability of HCC cells. Additionally, we measured ST6GAL1 expression in other HCC cell lines with different metastatic potentials. As shown in Fig. 1E, in contrast to the high expression of ST6GAL1 in non- or low-metastatic cell lines, metastatic cell lines expressed low or undetectable levels of ST6GAL1. These results suggest that ST6GAL1 may play a suppressive role in HCC metastasis.

Overexpression of ST6GAL1 inhibits HCC metastasis in vivo

To verify the role of ST6GAL1 in vivo, we established stable ST6GAL1-overexpressing HCCLM3 cells (ST6GAL1-OE). qRT-PCR, western blotting and flow cytometry confirmed high efficiency of ST6GAL1 expression in ST6GAL1-OE cells (Fig. 2A–C). We next examined the effects of ST6GAL1 on HCC growth using a xenograft and orthotopic cancer model. ST6GAL1-OE HCCLM3 cells and control HCCLM3 cells (Ctrl cells) were subcutaneously injected into nude mice, followed by the examination of tumor volumes every three days. High expression of ST6GAL1 inhibited tumor growth as seen by the significantly smaller volume of tumors derived from ST6GAL1-OE cells compared with tumors derived from control cells (Fig. 2D). To assess the effects of ST6GAL1 overexpression on HCC metastasis in vivo, equal volumes of the tumors obtained above were orthotopically implanted into the livers of nude mice. All mice were sacrificed after 40 days. As shown in Fig. 2E, intrahepatic metastases were observed in all mice implanted with HCCLM3 control cell derived tumors, whereas the ST6GAL1-OE group showed little intrahepatic metastasis in the orthotopic HCC implantation models ($n = 4$ per group, $p = 0.037$). Moreover, the nude mice injected with ST6GAL1-OE HCCLM3 cells developed smaller and fewer lung metastases compared with controls ($n = 10$ per group, $p = 0.002$) in a mouse tail vein metastasis model (Fig. 2F). Taken together, these results demonstrate that high expression of ST6GAL1 inhibits HCC metastasis in vivo.

ST6GAL1 is downregulated in HCC tissues and negatively correlates with tumor malignancy

To further explore ST6GAL1 expression in human HCC tissue and its correlation with the clinical phenotype, we performed immunohistochemical staining of tissue microarrays including 180 samples (88 paired HCC tumor and adjacent normal tissues and two paired intrahepatic cholangiocarcinoma (ICC) tumor and adjacent normal tissues). ST6GAL1 was scored from 0 to 12 by the staining intensity of immunohistochemistry. The correlation between ST6GAL1 expression and clinicopathological characteristics of HCC patients are summarized in Table 1. As shown in Fig. 3A, B, our data uncovered significantly lower expression of ST6GAL1 in tumors compared with matched normal liver tissues ($p < 0.001$). Moreover, the ST6GAL1 signal was almost absent in ICC cells compared with HCC cells. To clarify the clinical significance of ST6GAL1 downregulation in HCC, we analyzed the relationship between clinicopathological features and ST6GAL1 expression. As shown in Fig. 3A and Supplementary Fig. S1, tumor cells showed strong signals of ST6GAL1 in Golgi region (solid arrows) as well as in cytoplasm (dotted arrows) in stage I HCC. In stage II HCC, signal in Golgi region was still strong in almost all cells but the signal in cytoplasm was weakened. In contrast, in advanced-stage HCC (stage III and IV), only some or a few tumor cells had positive signals of ST6GAL1. Statistical analysis showed that ST6GAL1 expression was significantly negatively correlated with the TNM stage ($p < 0.001$) and vascular invasion ($p < 0.001$), and inversely associated with tumor differentiation ($p = 0.007$) (Fig. 3C–E). Additionally, we analyzed ST6GAL1 expression in HCC patients from The Cancer Genome Atlas (TCGA; $n = 347$) and GEO datasets GSE84005 ($n = 38$) cohort. Consistent with our results, ST6GAL1 was significantly downregulated in HCC tissues compared with normal tissues ($p < 0.001$ in TCGA cohort and $p = 0.003$ in the GSE84005 cohort), and negatively associated with TNM stages (Fig. 3F, G). Taken together, these data suggest that ST6GAL1 is significantly downregulated in HCC tissues and plays a suppressive role in HCC progression.

ST6GAL1 expression is associated with deregulation of cell migration and invasion in vitro revealed by glycoproteomic analysis

Next, to determine how ST6GAL1 plays a role in HCC metastasis, we used a metabolic labeling-based glycoproteomic strategy to reveal the potential functional alterations associated with ST6GAL1 expression. First, we performed metabolic labeling in control and ST6GAL1-OE HCCLM3 cells using $Ac_4ManNAz$. As shown in Fig. 4A, sialylated proteins were successfully labeled by azido sugars in both cell lines. After reacting with biotin-alkyne to complete click reaction, azido-tagged sialylated proteins on cell surface were enriched with streptavidin-beads and detected by mass spectrometry (MS) analysis. As a result, >2000 proteins were identified from both cells. Considering that sialic acids are typically found at the terminal position of N- and O-linked glycans attached to the cell surface and to secreted glycoproteins, we next mainly focused on cell membrane proteins. After TMHMM-2.0 analysis, 624 proteins were predicted to be membrane proteins. Among them, 336 with a fold change in relative expression ratio >2 between control and ST6GAL1-OE cells were considered to be differentially expressed proteins (Fig. 4B). Significantly perturbed

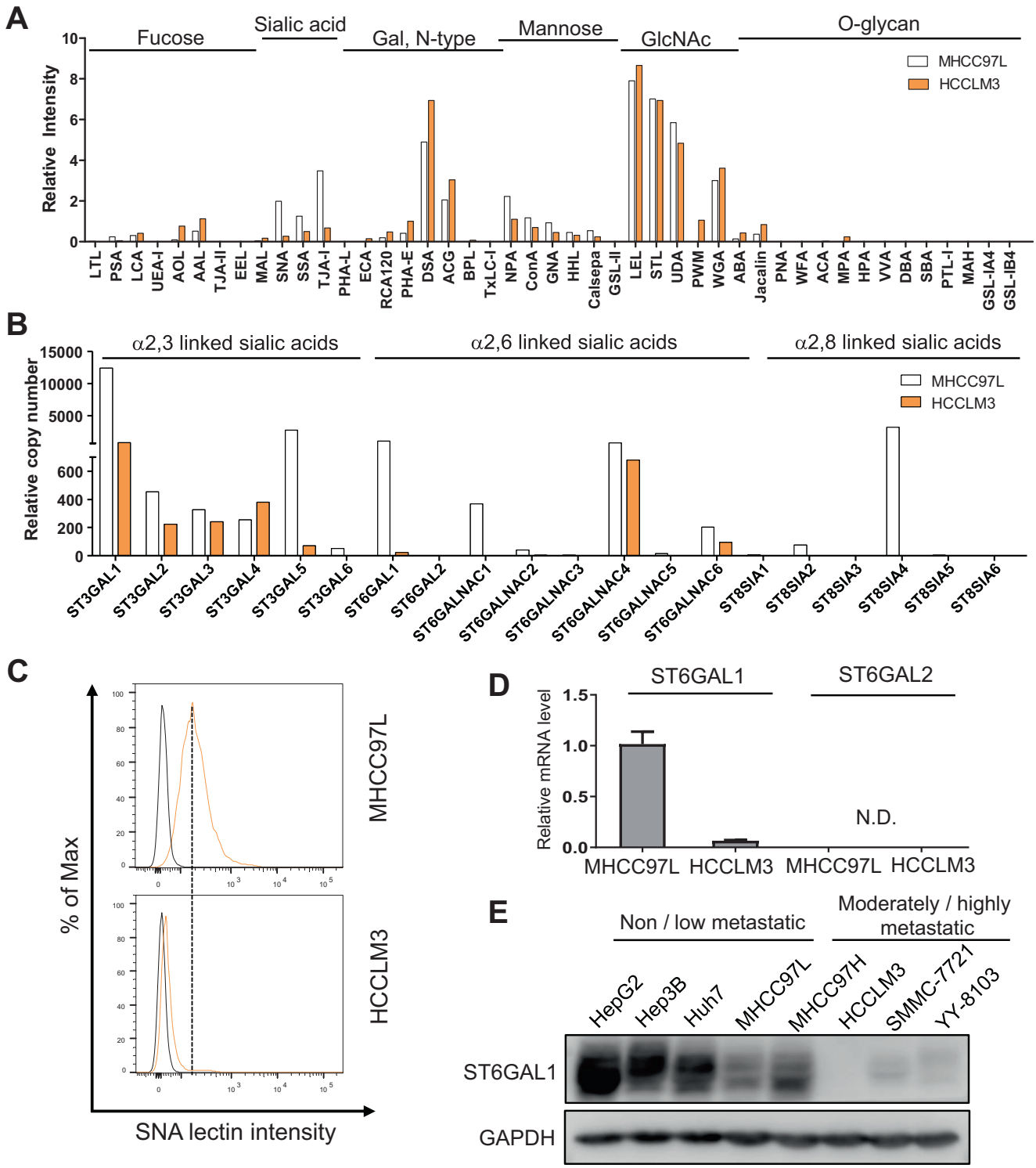

Fig. 1 The expression levels of cell surface α2,6 sialylation and the sialyltransferase ST6GAL1 are negatively correlated with the metastatic potentials of HCC cell lines. A Lectin microarray analysis of the membrane proteins from two different metastatic HCC cell lines, MHCC97L and HCCLM3, which have similar genetic background and different metastatic potentials (MHCC97L < HCCLM3). The signals of SNA, SSA and TJA-I that primarily recognize α2,6 sialylation were decreased in highly metastatic HCCLM3 cells compared with lowly metastatic MHCC97L cells. **B** TaqMan quantitative PCR assay showing the transcriptional levels of 20 different human sialyltransferases in the two cell lines. A sialyltransferase (ST6GAL1) mainly catalyzed α2,6 sialylation on N-glycans showed lower expression in highly metastatic HCCLM3 than in MHCC97L cells. **C** Cell surface α2,6 sialylation levels of HCCLM3 and MHCC97L cells were detected by flow cytometry using the lectin SNA. Both cells were incubated with biotinylated SNA and Alexa Fluor 488-conjugated streptavidin for detection. HCCLM3 showed lower α2,6 sialylation level on cell surface. **D** qRT-PCR analysis verified the low mRNA expression of ST6GAL1 in HCCLM3 cells. Data were shown as mean ± SD of three independent experiments. **E** Western blot analysis of ST6GAL1 expression in eight HCC cell lines were detected by anti-ST6GAL1 antibody. GAPDH was used as a loading control. SNA *Sambucus nigra* agglutinin, MAL *Maackia amurensis* lectin, SSA *Sambucus sieboldiana* agglutinin, TJA-I *Trichosanthes japonica* agglutinin-I, Gal galactose, GlcNAc N-acetylglucosamine.

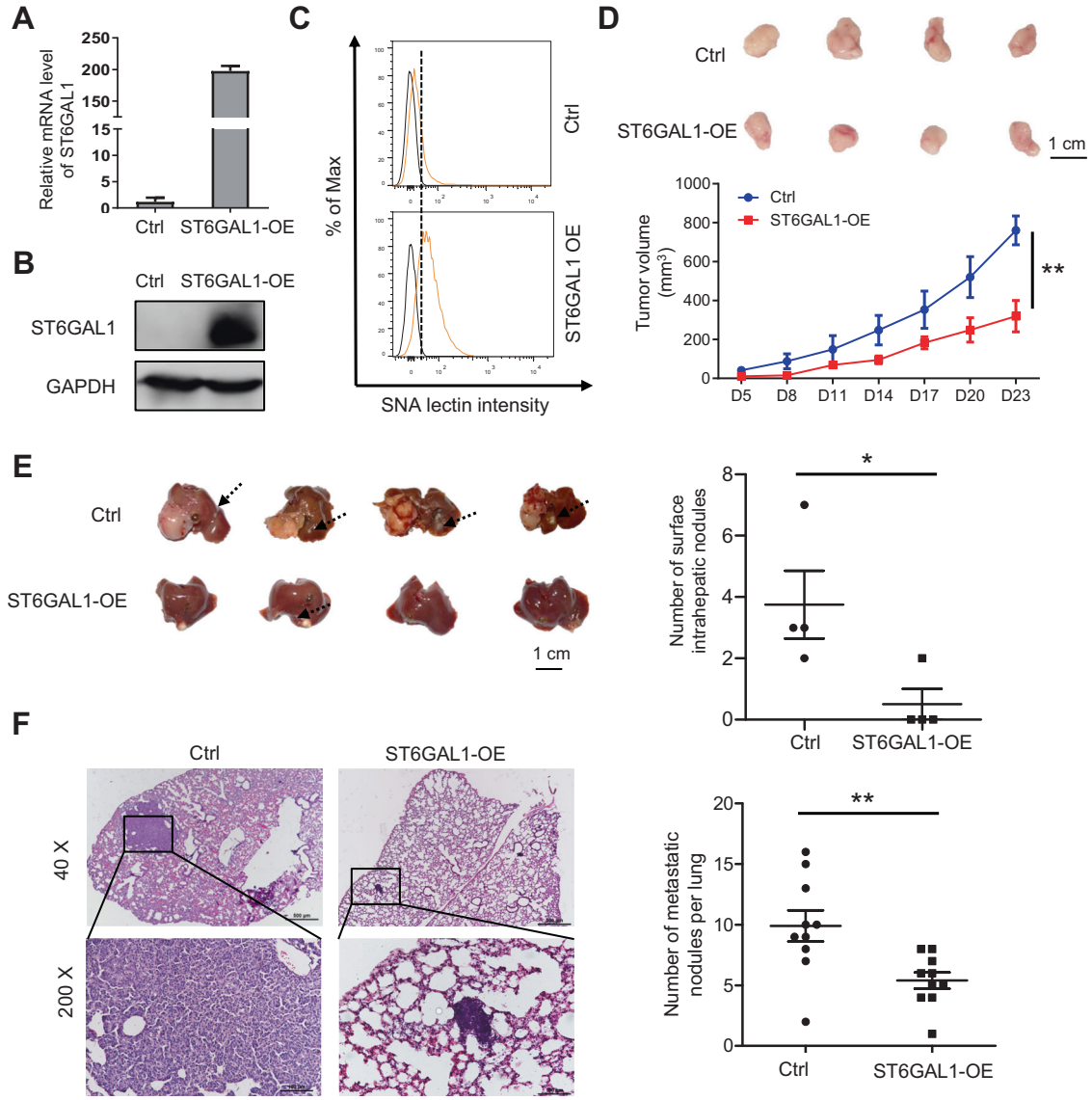

Fig. 2 ST6GAL1 overexpression inhibits HCC metastasis in vivo. Stable ST6GAL1 overexpressed HCCLM3 cell lines (ST6GAL1-OE HCCLM3) were generated. Relative mRNA expression and protein expression levels of ST6GAL1 in the indicated cells were detected by qRT-PCR (**A**) and western blotting (**B**), respectively. Data were shown as mean ± SD of three independent experiments. **C** Flow cytometry showed an increased level of cell surface α2,6 sialylation in ST6GAL1-OE HCCLM3 cells compared with relative control cells. The indicated cells were incubated with biotinylated SNA and detected by Alexa Fluor 488-conjugated streptavidin. **D** In vivo xenograft tumor-formation assays showed ST6GAL1 overexpression inhibited the tumor growth. ST6GAL1-OE and control HCCLM3 cells (2.5×10^6) were subcutaneously injected into the flanks of 5- to 6-weeks old male BALB/c nude mice, and tumor volumes (bottom) were measured every three days using precision calipers ($n = 4$ for each group). Data were shown as mean ± SEM. After four weeks post-injection, mice were sacrificed and tumors were collected and photographed (top). **E** In vivo orthotopic transplant model of HCC showed ST6GAL1 overexpression inhibited intrahepatic metastasis. Equal volumes of the tumors ($2 \times 2 \times 2$ mm) obtained above were orthotopically implanted into the livers of 5- to 6-weeks old male BALB/c nude mice ($n = 4$ for each group). After 40 days post-injection, mice livers were collected and the intrahepatic metastasis nodules were indicated by dotted arrows. The number of intrahepatic foci in each group was calculated. Data were shown as mean ± SEM. **F** H&E staining of lung tissues showed ST6GAL1 overexpression inhibited lung metastasis of HCC. ST6GAL1-OE and control HCCLM3 cells (2×10^6) were injected into the tail vein of 5- to 6-weeks old male BALB/c nude mice ($n = 10$ for each group). After eight weeks, the lungs were collected and the number of lung metastatic nodules in each group was calculated. Data were shown as mean ± SEM. Statistical analysis was performed using paired two-tailed Student's *t* tests (**D**) and unpaired two-tailed Student's *t* tests (**E** and **F**). $^*p < 0.05$; $^{**}p < 0.01$. SNA *Sambucus nigra* agglutinin, Ctrl control HCCLM3 cells, ST6GAL1-OE the ST6GAL1-overexpressing HCCLM3 cells.

functions (activation z-score >2 or <−2) of these proteins assessed by Ingenuity Pathways Analysis (IPA) were shown in Fig. 4C. Interestingly, functions associated with cell motility, such as cell migration and cell movement, were all consistently downregulated after overexpression of ST6GAL1 (dark blue columns in Fig. 4C). To verify these predictions, we performed cell migration and invasion assays. Consistently, ST6GAL1 overexpression resulted in a significant reduction of cell migration ($p = 0.001$, Fig. 4D) and invasion ($p = 0.007$, Fig. 4D). These results indicate that high expression of ST6GAL1 may suppress HCC metastasis by inhibiting the migratory ability of tumor cells in vitro.

To further determine critical proteins that mediate ST6GAL1 functions in HCC metastasis, we repeating the metabolic labeling-based proteomic analysis in MHCC97L and HCCLM3 cells with different metastatic potentials and ST6GAL1 expression. We first confirmed that the migratory and invasive abilities of MHCC97L with

Table 1. The correlation between ST6GAL1 expression and clinicopathological characteristics of HCC patients.

Characteristics	Number of patients (%)	Tumor ST6GAL expression (IHC socres)[a]	*p* value[b]
Age, year			0.088
≤50	55 (62.5%)	6.4 ± 2.5	
>50	33 (37.5%)	5.4 ± 2.2	
Gender			0.247
Male	82 (93.2%)	6.0 ± 2.4	
Female	6 (6.8%)	7.3 ± 3.3	
HBsAg			0.349
Negative	18 (20.5%)	5.5 ± 2.2	
Positive	70 (79.5%)	6.2 ± 2.5	
Cirrhosis			0.803
Absent	43 (48.9%)	6.2 ± 2.7	
Present	45 (51.1%)	5.9 ± 2.2	
Tumor size, cm			**0.003**
≤5	35 (39.8%)	7.0 ± 2.2	
>5	53 (60.2%)	5.4 ± 2.4	
Vascular invasion			**<0.001**
Absent	49 (55.7%)	6.9 ± 2.2	
Present	39 (44.3%)	4.9 ± 2.4	
Intrahepatic metastasis			**0.009**
No	70 (79.5%)	6.4 ± 2.4	
Yes	18 (20.5%)	4.7 ± 2.2	
TNM stage			**<0.001**
I	40 (45.5%)	7.2 ± 2.1	
II	17 (19.3%)	6.1 ± 2.3	
III	26 (29.5%)	4.5 ± 2.1	
IV	5 (5.7%)	4.4 ± 2.2	
Tumor differentiation			**0.007**
Well	2 (2.3%)	8.5 ± 0.5	
Moderate	59 (67.0%)	6.5 ± 2.5	
Poor	27 (30.7%)	4.9 ± 2.2	

[a]The data were shown as mean ± SD.
[b]The results were analyzed by Mann–Whitney *U*-test or Kruskal-Wallis test.
p values in bold denote statistical significance.

a high expression of ST6GAL1 were significantly lower compared with those of HCCLM3 cells (Supplementary Fig. S2A, B). The high labeling efficiency of sialylated proteins by Ac_4ManNAz metabolic labeled in both cells was shown in Fig. 4E. Next, we compared the differentially expressed membrane proteins in ST6GAL1-OE *v.s.* Ctrl HCCLM3 group and MHCC97L *v.s.* HCCLM3 group, and searched for proteins involved in cell motility with the same expression trend in the two groups as the potential substrates of ST6GAL1. As shown in Fig. 4F, 77 of the 336 differentially expressed proteins in the ST6GAL1-OE *v.s.* Ctrl HCCLM3 group were related to cell motility. Fifteen of them were confirmed to be expressed on the plasma membrane by Uniprot annotation and GO analysis (Cellular component) and had consistent expression trends in the MHCC97L *v.s.* HCCLM3 group (Fig. 4G), indicating the possible involvement of these proteins in ST6GAL1 functions in HCC metastasis.

ST6GAL1 overexpression impaires the dimerization of MCAM and decreases its expression on cell surface

Among these potential candidates, we focused on those with N-glycans modification (Fig. 4G) and validated the expression of some proteins by western blotting (Supplementary Fig. S3). In particular, downregulated MCAM after ST6GAL1 overexpression attracted our attention because this molecule has been reported to be critical for HCC metastasis [20, 21] and there is evidence of its contribution to tumor angiogenesis [22]. Thus, to examine whether ST6GAL1 exerted its functions in HCC metastasis partially by regulating MCAM expression, we first confirmed the MS results by western blot analysis. Consistently, MCAM was clearly decreased in ST6GAL1-OE cells as compared with control cells (Fig. 5A). Additionally, lectin flow cytometry (Fig. 5B) and immunofluorescence staining (Fig. 5G) further demonstrated a reduction of MCAM on cell surface. Despite the decreased expression at the protein level, interestingly, the mRNA level of MCAM after ST6GAL1 overexpression showed no significant difference (Fig. 5C), indicating post-transcriptional regulation of MCAM expression by ST6GAL1. Considering that MCAM in cell lysate exists primarily as a dimer [23], we further assessed the expression of MCAM dimers and found ST6GAL1 overexpression caused a marked reduction in MCAM dimerization (Fig. 5D). Recently, it is reported that extracellular galectin-3 binds to N-glycans on MCAM and induces MCAM dimerization on cell surface and its subsequent activation of cell signaling [24]. Considering that α2,6 sialylation but not α2,3 sialylation inhibits the interaction between galectin-3 and N-glycans [25, 26], we were wondering whether the downregulated MCAM dimers in ST6GAL1-OE cells were due to its increased α2,6 sialylation and reduced interaction with galectin-3. To test this, we first performed a co-immunoprecipitation assay. Overexpression of ST6GAL1 clearly increased reactivity of MCAM with SNA, but decreased its reactivity with MAL, suggesting enhanced α2,6 sialylation on MCAM (Fig. 5E). Consistent with this observation, the interaction between MCAM and galectin-3 was substantially attenuated after ST6GAL1 overexpression (Fig. 5F). Furthermore, strong cell-surface co-localization of MCAM with exogenous galectin-3 was observed in control but not in ST6GAL1-OE cells (Fig. 5G). Finally, we examined the expression profile of MCAM and galectin-3 in different HCC cell lines. Interestingly, both galectin-3 and MCAM were highly expressed in highly metastatic HCC cells with low ST6GAL1 expression, but weakly expressed in non-metastatic cells with high ST6GAL1 expression (Supplementary Fig. S4). These results clearly showed that ST6GAL1 can affect the expression and interaction of MCAM by regulating its sialylation.

ST6GAL1 exerts its function in HCC metastasis by regulating MCAM expression

To further validate whether ST6GAL1 exerts its function in HCC metastasis by regulating MCAM expression, we generated two stable MCAM knockdown cells with independent target sequences of MCAM in ST6GAL1-deficient HepG2 cells. ST6GAL1 and MCAM expression levels in indicated cells were assessed by western blot analysis (Fig. 6A). In in vitro Transwell assays, knockdown of MCAM significantly reduced the enhanced migratory and invasive abilities of HepG2-shST6GAL1 cells ($p < 0.001$) (Fig. 6B, C). In in vivo tumor metastasis model by tail vein injection, HepG2-shST6GAL1 developed bigger and more lung metastases compared with the controls, whereas knockdown of MCAM in HepG2-shST6GAL1 cells significantly abolished the increased incidence and volume of lung metastases of HCC ($p < 0.001$) (Fig. 6D, E). These results indicate that MCAM is one of the essential substrate glycoproteins for ST6GAL1 to exert its functions in HCC metastasis.

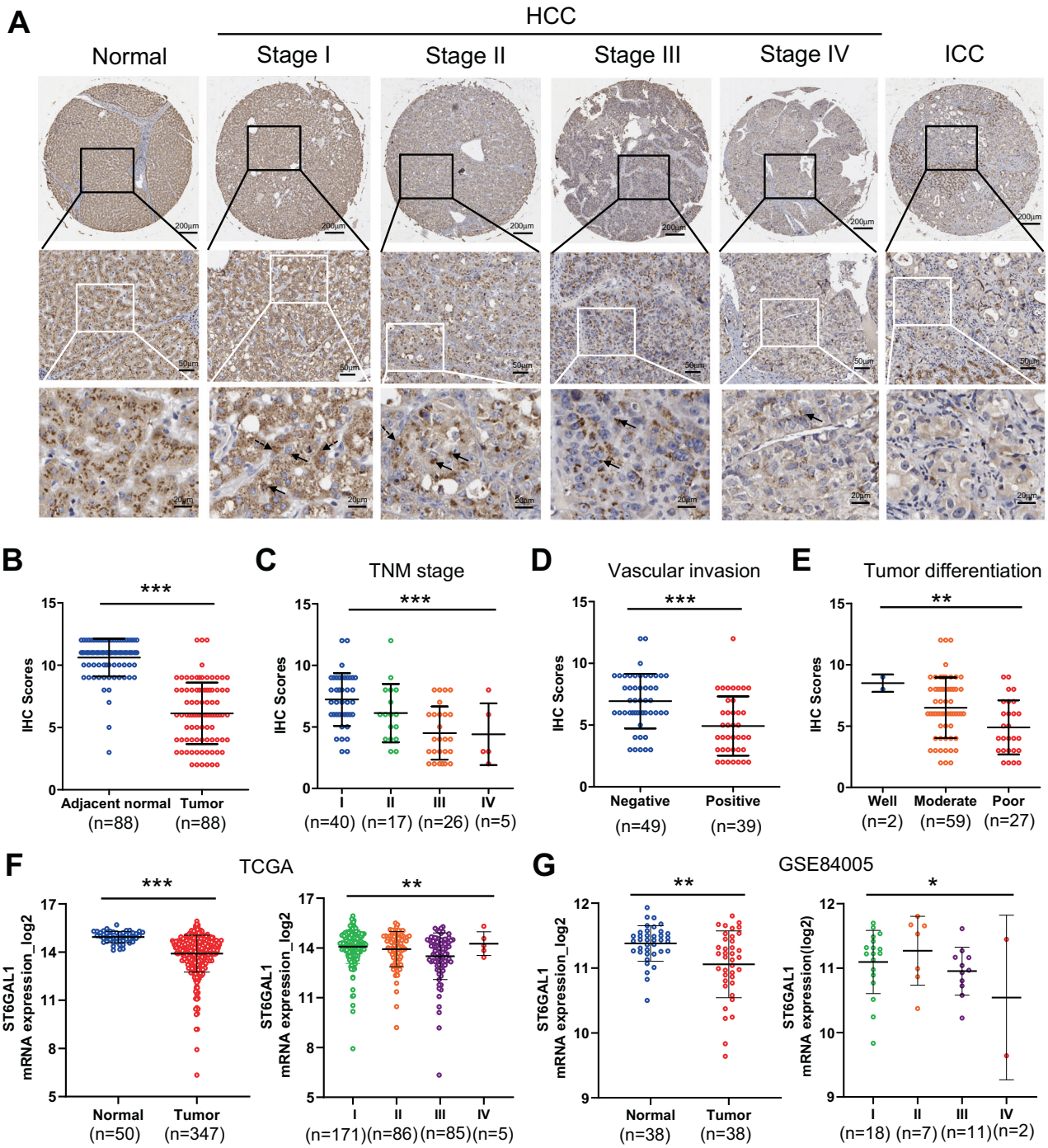

Fig. 3 ST6GAL1 is downregulated in human HCC tissues and its expression is negatively correlated with TNM stages, vascular invasion and tumor differentiation of HCC. A Immunohistochemical (IHC) staining of ST6GAL1 was performed in 180 tissue samples (88 paired HCC tumor and adjacent normal tissues and 2 paired intrahepatic cholangiocarcinoma (ICC) tumor and adjacent normal tissues). Representative pictures of each stage showed ST6GAL1 could expressed both in the Golgi region (solid arrows) and cytoplasm (dotted arrows) in HCC tumors. The IHC score was evaluated by calculating the product of staining intensity and staining area with a range of 0–12, as described in Materials and Methods. **B** Protein levels of ST6GAL1 were significant decreased in HCC tissues compared with paired normal hepatic tissues. ST6GAL1 were significantly negatively associated with TNM stage (**C**), vascular invasion (**D**) and tumor differentiation (**E**) of HCC. mRNA expression levels of ST6GAL1 were significant decreased in HCC tissues and negatively associated with TNM stages in the TCGA database containing 347 HCC tumors and 50 normal tissues (**F**) as well as in the GSE84005 database containing paired 38 HCC tumors and normal tissues (**G**). All data were shown as mean ± SD. Statistical analysis was performed using two-tailed Mann–Whitney *U*-tests (**B**, **D**, **F** and **G**) and two-tailed Kruskal-Wallis test (**C**, **E**–**G**). *$p < 0.05$; **$p < 0.01$; ***$p < 0.001$.

Expression and prognostic value of sialylated MCAM in HCC tissues

To determine the clinical significance of sialylated MCAM in HCC, we examined the expression of relative intensities of sialylated MCAM in HCC tumor tissues from two cohorts by SNA immunoprecipitation (Fig. 7A). As a result, it showed a negative correlation with TNM stages ($p = 0.089$, Fig. 7B) and vascular invasion ($p = 0.016$, Fig. 7C) of HCC patients. Furthermore, Kaplan-

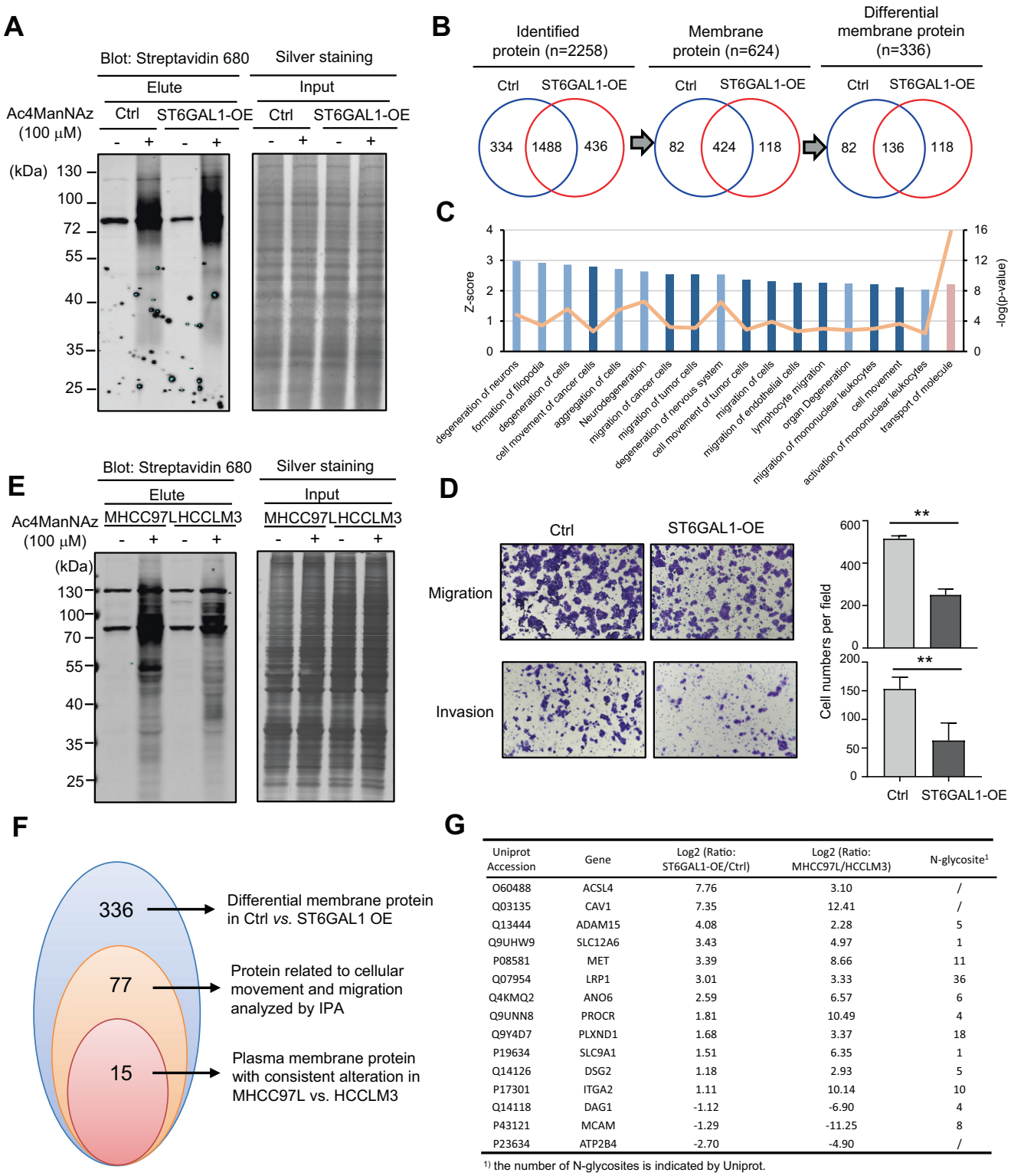

G

Uniprot Accession	Gene	Log2 (Ratio: ST6GAL1-OE/Ctrl)	Log2 (Ratio: MHCC97L/HCCLM3)	N-glycosite[1]
O60488	ACSL4	7.76	3.10	/
Q03135	CAV1	7.35	12.41	/
Q13444	ADAM15	4.08	2.28	5
Q9UHW9	SLC12A6	3.43	4.97	1
P08581	MET	3.39	8.66	11
Q07954	LRP1	3.01	3.33	36
Q4KMQ2	ANO6	2.59	6.57	6
Q9UNN8	PROCR	1.81	10.49	4
Q9Y4D7	PLXND1	1.68	3.37	18
P19634	SLC9A1	1.51	6.35	1
Q14126	DSG2	1.18	2.93	5
P17301	ITGA2	1.11	10.14	10
Q14118	DAG1	-1.12	-6.90	4
P43121	MCAM	-1.29	-11.25	8
P23634	ATP2B4	-2.70	-4.90	/

[1] the number of N-glycosites is indicated by Uniprot.

Meier analysis of overall survival in 370 HCC samples from TCGA database showed that the prognostic value of MCAM ($p = 0.134$, Fig. 7D) or ST6GAL1 ($p = 0.059$, Fig. 7E) alone was not sufficient. However, when using a binary logistic regression model combined with MCAM and ST6GAL1 (y = 0.197*MCAM-0.168*ST6GAL1-0.210), the combined index showed better performance in HCC prognosis ($p = 0.002$, Fig. 7F). Taken together, these results suggest that sialylated MCAM in HCC tissues plays an inhibitory role in tumor progression, and has better prognostic value than MCAM protein itself in HCC patients.

DISCUSSION

Altered sialylation has long been associated with tumor progression and metastasis because of aberrant expression of certain sialyltransferases or sialidases [27]. In the current study, we found

Fig. 4 Discovery of substrate proteins of ST6GAL1 by metabolic labeling-based glycoproteomic analysis. A Glycoproteomic analysis of metabolic labeled sialylated proteins in ST6GAL1-OE and control HCCLM3 cells. The indicated cells were cultured with 100 μM of Ac_4ManNAz or ManNAc (negative control) for 60 h. The cell lysates were click reacted with biotinylated alkyne and labeled glycoprotein were enriched by streptavidin-agarose beads. Eluted proteins were immunoblotted with streptavidin-680 to detected the labeling efficiency. Input cell lysates detected by silver staining were used as loading control between different groups. **B** Venn plot showed differentially expressed proteins between control and ST6GAL1-OE cells. A total of 2258 proteins were identified by mass spectrometry analysis, of which 624 were predicted as membrane proteins using TMHMM-2.0. Among these proteins, 336 with a fold change in relative expression ratio >2 between control and ST6GAL1-OE cells were considered as differentially expressed proteins. **C** IPA analysis of these 336 proteins showed significantly up-regulated (activation z-score > 2) and down-regulated functions (activation z-score < −2) caused by ST6GAL1 overexpression. red, up-regulated functions; blue, down-regulated functions; dark blue, down-regulated functions related to cell migration and cell movement. **D** Transwell analysis verified the down-regulated migratory ability and invasive ability of ST6GAL1-OE HCCLM3 cells. Data were shown as mean ± SD of three independent experiments. Statistical analysis was performed using unpaired two-tailed Student's *t* tests. $^{**}p < 0.01$. **E** Metabolic labeling efficiency of cell surface sialylated proteins with Ac4ManNAz in MHCC97L cells and HCCLM3 cells. Eluted proteins were immunoblotted with streptavidin-680 and input cell lysates detected by silver staining. **F** A total of 336 proteins were identified as differentially expressed proteins in ST6GAL1-OE *v.s.* Ctrl HCCLM3 group, of which 77 were related to cell motility by IPA analysis. Among these proteins, 15 proteins showing consistent expression trends in MHCC97L *v.s.* HCCLM3 group were considered as potential substrate proteins that mediated ST6GAL1 functions in HCC migration and invasion. **G** Information of these 15 proteins were shown. Ctrl control HCCLM3 cells, ST6GAL1-OE the ST6GAL1-overexpressing HCCLM3 cells.

that the sialyltransferase ST6GAL1 was significantly downregulated in HCC cells and negatively correlated with the metastatic potentials of HCC cells and adverse clinicopathological features of HCC tissues. Overexpression of ST6GAL1 inhibited migration and invasion of HCC cells in vitro and suppressed HCC metastasis in vivo. Importantly, we identified MCAM as an important substrate glycoprotein regulated by ST6GAL1 using a metabolic labeling glycoproteomic strategy. Overexpression of ST6GAL1 increased α2,6 sialylation on MCAM, which suppressed the interaction between MCAM and galectin-3, and thus impair the dimerization of MCAM on cell surface and subsequent HCC metastasis (Fig. 7G). Taken together, our data demonstrate that ST6GAL1 might play a suppressive role in HCC metastasis by regulating MCAM expression, which provides a novel insight into the mechanistic role of ST6GAL1 in tumor malignancy.

In recent years, ST6GAL1 has become the most well-described sialyltransferase in the literature [10]. This study provides both in vitro and in vivo evidence that ST6GAL1 is a tumor metastasis suppressor of HCC. Supporting our findings, decreased tumor ST6GAL1 activity was shown to lead to poor prognosis of HCC patients [28]. Another study of 21 HCC tissues also reported that ST6GAL1 expression was influenced by the tumor grade, with lower expression in HCC of grade 3–4 than in grade 2 HCC [29]. It is interesting to note that in previous studies, ST6GAL1 was generally thought to be associated with more invasive and metastatic progression of many types of cancer [11–16], except for bladder cancer and glioblastoma in which ST6GAL1 was downregulated in advanced tumor grade and decreased cell invasion and tumor growth [30–32]. Our study provides another example of ST6GAL1 as an inhibitor of tumor development. In fact, although many studies have shown positive associations between ST6GAL1 expression and tumor progression in colon cancer [15, 33, 34], the opposite role of ST6GAL1 inhibiting tumor metastasis has also been shown in the same type of cancer [35–37]. Overall, these data suggest that ST6GAL1 plays distinctive roles in a cancer type- and tissue type-specific manner.

Currently, it is still unclear why ST6GAL1 has cancer type-specific functions in tumor progression. However, we speculate that the negative correlation of ST6GAL1 expression with HCC progression may be related to the following reasons. (1) It is well known that ST6GAL1 has tissue-specific expression in humans. Compared with other epithelial tissues, ST6GAL1 expression is very high in the liver. Our immunohistochemistry results and TCGA data (Fig. 3) also confirmed that ST6GAL1 was highly expressed in the normal liver at both mRNA and protein levels. Although the molecular functions of highly expressed ST6GAL1 in the liver are unclear, a recent study showed that it is likely related to helping maintain systemic immunity in the liver [38]. Using a mouse model with hepatocyte-specific ablation of ST6GAL1, they found that loss of hepatocyte α2,6 sialylation induced a proinflammatory state and increased systemic immune responses [38]. We believe this finding may partly explain that the downregulated expression of ST6GAL1 in HCC may be related to disruption of immune homeostasis. (2) Recently, Bellis et al. summarized the current knowledge regarding the genetic, epigenetic, transcriptional, and posttranslational regulatory mechanisms responsible for ST6GAL1 expression in cancer cells [39]. Notably, hypermethylation of the P3 promoter decreased expression of ST6GAL1 in bladder and glioblastoma cancer cells [30, 40]. Therefore, there may be other epigenetic regulation on the ST6GAL1 promoter, which causes its downregulation during HCC progression. (3) Additionally, our lectin array results showed that, in contrast to the decreased reactivity to lectins recognizing α2,6 sialylation (SNA, SSA, and TJA-1), the intensities of lectins recognizing fucosylation (AOL, AAL, and LCA) were consistently higher in highly metastatic HCC cell lines (Fig. 1). The opposite expression tendency between α2,6 sialylation and fucosylation in cells does not appear to be random, because recent studies have shown that a reduction in α2,6 sialylation is accompanied by increased core fucosylation in rheumatoid arthritis patient serum [41] and inhibition of fucosylation in HepG2 cells dramatically increases α2,6 sialylation [42]. Therefore, we speculate that downregulation of ST6GAL1 and α2,6 sialylation in HCC cells may favor tumor metastasis, because it will increase the level of fucosylation that has been reported to promote the progression and metastasis of HCC [43].

As a glycosyltransferase, the function of ST6GAL1 is to regulate the degree of α2,6 sialylation on various glycoproteins, thereby affecting cellular behaviors. For example, ST6GAL1 affect cell invasion, migration, and apoptosis by altering sialylation of integrins, EGFR, TNFR, and FasR [11, 17, 18, 44]. Therefore, discovery of substrate proteins is particularly important to understand the molecular mechanism of ST6GAL1 functions. In this study, we systematically revealed a series of protein candidates that may be regulated by ST6GAL1 during HCC progression using a metabolic labeling glycoproteomic strategy. Furthermore, we demonstrated that high expression of α2,6 sialylation on MCAM regulated by ST6GAL1 inhibited its interaction with galectin-3 and suppressed its dimerization on cell surface (Fig. 5). Knockdown of MCAM abrogated the enhanced HCC migratory and metastatic abilities driven by ST6GAL1 deficiency (Fig. 6). MCAM has been reported to promote cell migration and invasion, and is involved in HCC metastasis [20]. The dimeric form of MCAM on cell surface plays important roles in outside-in signal transduction [45] and is associated with tumor malignancy [46]. In particular, galectin-3 binds to MCAM and induces its dimerization and subsequent activation of protein kinase B (AKT) signaling [24], which is

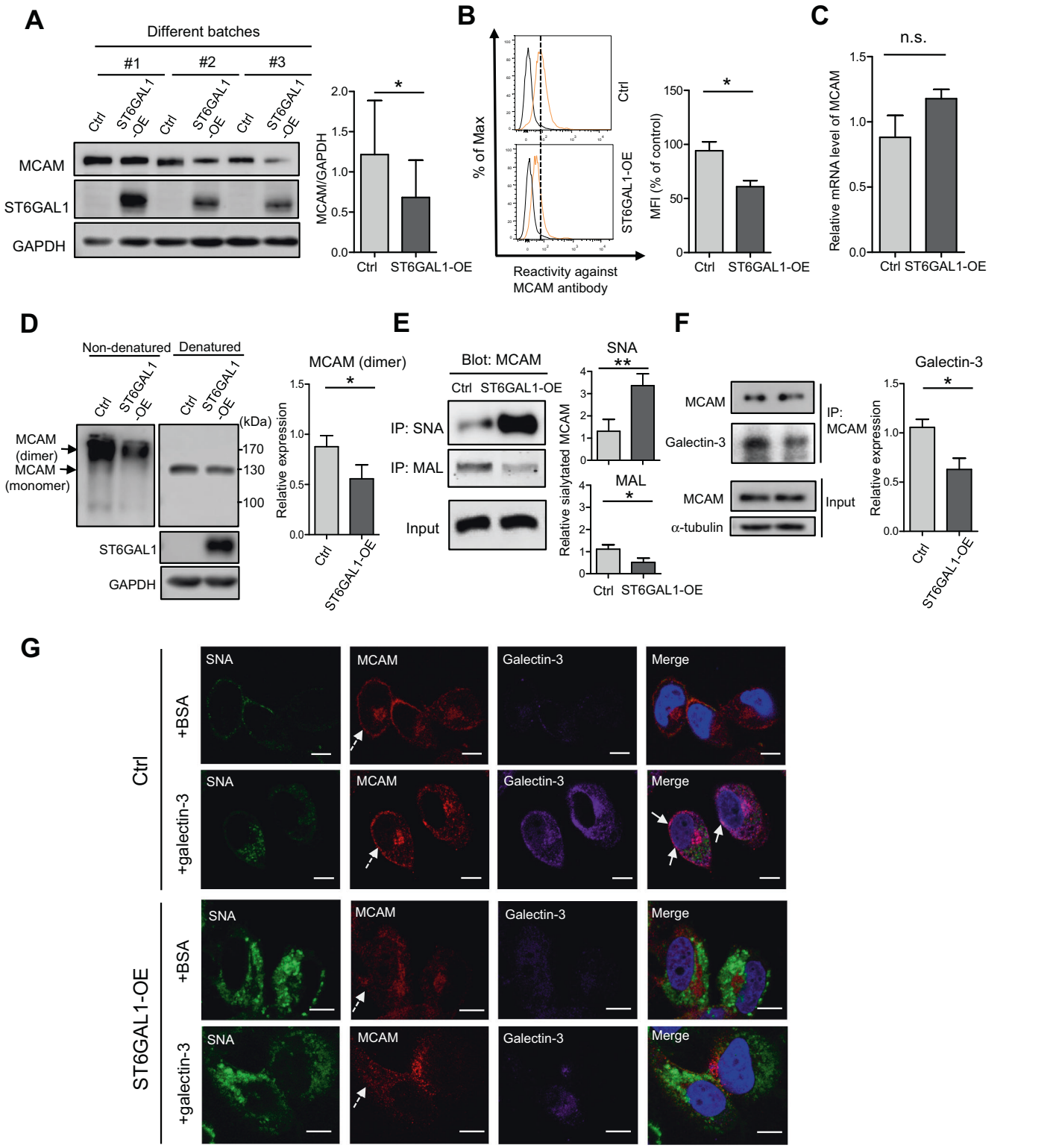

important for HCC tumorigenesis [21]. Therefore, it is conceivable that ST6GAL1 may inhibit the migration and invasion of HCC cells partially via MCAM. Additionally, ST6GAL1-mediated sialylation appears to inhibit VEGF-independent angiogenesis [47], whereas soluble MCAM has been shown to contribute to tumor angiogenesis [22]. Because the expression of membrane MCAM in cancer cells is closely associated with secretion of soluble MCAM [22], in addition to the inhibitory effects on cell migration and invasion, we postulate that high expression of ST6GAL1 may also impair tumor vascularization by regulating MCAM dimerization during HCC metastasis. Obviously, it should be noted that ST6GAL1 affects HCC metastasis by regulating the level of α2,6 sialylation on many substrate proteins. In this study, we used MCAM as an example for verification and further study of other proteins is needed to unravel the cancer type specificity and complex activities of ST6GAL1 in HCC.

Fig. 5 ST6GAL1 overexpression decreases the expression of MCAM, impairs its interaction with galectin-3 and dimerization on cell surface. A Western blot analysis showed decreased protein expression levels of MCAM in ST6GAL1-OE HCCLM3 cells compared with control cells. GAPDH was used as a loading control. **B** Flow cytometry analysis verified a decreased level of cell surface MCAM in ST6GAL1-OE HCCLM3 cells. The indicated cells were incubated with anti-MCAM antibody and detected by Alexa Fluor 488-conjugated goat anti-rabbit IgG. **C** qRT-PCR analysis showed the mRNA expression of MCAM in both cells. **D** Western blot analysis of cell lysates from the indicated cells under non-denatured or denatured gel electrophoresis were detected by anti-MCAM antibody. Native Page (left) showed a decreased level of MCAM dimers. **E** Lectin immunoprecipitation analysis showed increased α2,6 sialylation but decreased α2,3 sialylation on MCAM in ST6GAL1-OE cells. Cell lysates from the indicated cells were incubated with SNA- or MAL-agarose beads. The immunoprecipitates were eluted and immunoblotted with anti-MCAM antibody. **F** Anti-MCAM co-immunoprecipitation assay showed decreased levels of galectin-3 interacting with MCAM in ST6GAL1-OE cells. Cell lysates were incubated with anti-MCAM antibody and the elute was detected by anti-galectin-3 antibody. **G** Immunofluorescence staining verified the decreased level of MCAM on cell surface and the weaker interaction between MCAM and extracellular galectin-3 in ST6GAL1-OE cells. The indicated cells were treatment with BSA (2 μg/mL) or with recombinant galectin-3 (2 μg/mL) for 1 h, the cells were immunostained with FITC-conjugated SNA (green), anti-MCAM and Alexa Fluor 594-conjugated secondary antibody(red), and anti-Galectin-3 and Alexa Fluor 647-conjugated secondary antibody (purple), respectively. Cell nuclei were stained by DAPI (blue). Dotted arrow indicated the level of MCAM on cell surface and solid arrows indicated the signals of MCAM merging with Galectin-3 (pink). Scale bars, 10 μm. All data were shown as mean ± SD. Statistical analysis was performed using paired two-tailed Student's *t* tests (**A**) and unpaired two-tailed Student's *t* tests (**B**–**F**). $*p < 0.05$; $**p < 0.01$; n.s., not significant. SNA *Sambucus nigra* agglutinin, MAL *Maackia amurensis* lectin, Ctrl control HCCLM3 cells, ST6GAL1-OE the ST6GAL1-overexpressing HCCLM3 cells.

Liver is an organ with high expression of sialic acid. Our study demonstrated a novel tumor metastasis inhibitor role of ST6GAL1 in HCC by regulating MCAM expression on cell surface, which is different with previous studies in many other types of cancers, and supports the functional complexity of ST6GAL1 in a cancer type- and tissue type-specific manner. Notably, both ST6GAL1 and MCAM have their own soluble forms and are detectable in the serum of HCC patients. Therefore, it is possible that the levels of soluble ST6GAL1/MCAM in serum may serve as a biomarker for the poor prognosis of HCC patients.

MATERIALS AND METHODS

Cell lines, cell culture and stable cell lines construction

The 293T cell line was purchased from ATCC (Manassas, VA, USA). Hep3B, Huh7, SMMC-7721, YY-8103, HepG2, MHCC97L, MHCC97H and HCCLM3 cell lines were gifts from Dr. Xin Zhang (The Second Military Medical University, China). MHCC97L, MHCC97H and HCCLM3 are metastatic cell lines with similar genetic background because they are subclones sequentially isolated from a MHCC97 parental cell line through in vivo selection [19]. The metastatic potentials of these three cell lines are gradually increased, among which MHCC97L has the lowest metastatic potential and HCCLM3 has the highest metastatic potential. In the spontaneous metastasis models via orthotopic implantation, HCCLM3 caused widespread loco-regional and distant metastases including 100% pulmonary metastases, 100% intrahepatic metastases, 80% intra-abdominal cavity metastases, and 70% diaphragm metastases, while MHCC97L only caused 40% pulmonary metastases. In addition, in the spontaneous metastasis models via subcutis inoculation, the pulmonary metastatic rate of HCCLM3 was 100%, while that of MHCC97L was zero.

The 293 T cell line was cultured in high glucose Dulbecco's modified Eagle's medium (DMEM) with 2 mM L-glutamine and 10% fetal bovine serum (FBS). Other cell lines were maintained in high glucose DMEM with 10% FBS. All cells were cultured in a humidified atmosphere containing 5% CO_2 at 37 °C.

ST6GAL1 overexpressing and knockdown cells were established as described previously [13, 48]. To stably knockdown MCAM in HepG2 cells, small-hairpin RNA was designed and inserted into GV493 vector (Genechem, Shanghai, China). A scramble shRNA was used as negative control. The shMCAM plasmids were co-transfected into HEK293T cells with packaging plasmid psPAX2 and envelope plasmid pMD2.G using Lipo-2000 (Thermo Fisher Scientific). Lentivirus were harvested 48 h after transfection and filtered through 0.45 μm PVDF filters. HCCLM3 and HepG2 cells were seeded in 6-well plates at a density of 5×10^5 cells per well and grown to 50% confluence on the day of lentivirus infection. The stable cell lines were obtained by antibiotic selection (puromycin 3 μg/mL). The shMCAM target sequences were as follows: shMCAM#1: 5′-GTGTTGAATCTGTCTTGTGAA-3′; shMCAM#2: 5′-AGTTGAAGTTAAGTCAGATAA-3′.

In vivo metastasis assays

Male BALB/c nude mice (5- to 6-weeks old, weighting 20–22 g) were obtained from the Shanghai Institute of Materia Medica, Chinese Academy of Science. All studies on mice were conducted in accordance with the National Institutes of Health "Guide for the Care and Use of Laboratory Animals" and were approved by the Institutional Animal Care and Use Committee of Shanghai Jiao Tong University. For the orthotopic HCC implantation model, 2.5×10^6 cells in fresh medium were injected subcutaneously to obtain subcutaneous tumors. After four weeks, the mice were sacrificed to obtain the HCC tissues. The xenograft HCC model was established by orthotopic inoculation of histologically intact tumor tissue (2 × 2 × 2 mm) into the livers of nude mice. Each group contained four mice. Forty days later, the mice were sacrificed and the number of intrahepatic metastatic nodules were counted. For the tumor metastasis model, 2×10^6 cells in 200 μL PBS were injected into the tail vein of the mice. Mice were randomly and blindly divided into several groups ($n = 10$ per group in HCCLM3 groups and $n = 5$ per group in HepG2 groups). After eight weeks, the mice were sacrificed and the lungs were excised and embedded in paraffin. Metastatic lung foci were confirmed by hematoxylin and eosin staining.

Tissue microarray and immunohistochemistry (IHC)

A tissue microarray was constructed as described previously [49], which contains 88 matched pairs of HCC and two matched pairs of ICC tumor (odd columns) and normal (even columns) samples. Written informed consent was obtained from all patients and the procedure was approved by the Ethics Committee of Eastern Hepatobiliary Surgery Hospital.

Tissue array sections (4 μm) were deparaffinized and dehydrated, and then treated with 3% H_2O_2 at room temperature for 15 min to block endogenous peroxidase activity. After antigen retrieval in citrate buffer, the slides were incubated with anti-ST6GAL1 antibody (1:200, R&D Systems, Minneapolis, MN, USA) overnight at 4 °C. Staining was performed with 3,3-diaminobenzidine (DAB) and counterstaining with hematoxylin. The intensity score of staining was categorized into 0, 1, 2, or 3, denoting negative, weak, moderate, or strong staining, respectively. Scoring was conducted by the percentage of positive-staining cells: 0–5% scored 1, 6–35% scored 2, 35–70% scored 3, and >70% scored 4. The immunostaining score was calculated by the intensity score × the percentage score.

Western blotting and immunoprecipitation

For western blotting, cells were washed with PBS, lysed with lysis buffer (10 mM Tris-HCl, 1% Triton X-100, and 150 mM NaCl), and centrifugated at 15,000 rpm for 10 min at 4 °C. Equal amounts of proteins were separated by SDS-PAGE at the appropriate concentration, transferred to nitrocellulose membrane, and probed with the appropriate antibodies, or with biotinylated SNA, MAL (Vector Laboratories, Burlingame, CA, USA). Primary antibodies included anti-ST6GAL1 antibody (1:500; R&D Systems), anti-MCAM antibody (1:1000; CST, Danvers, MA, USA), anti-galectin-3 antibody (1:1000; CST), anti-CAV1 antibody (1:2000; ABclonal, Wuhan, China), anti-MET antibody (1:2000; ABclonal), anti-ADAM15 antibody (1:1000; ABclonal), anti-DSG2 antibody (1:2000; ABclonal), anti-DAG1 antibody (1:1000; ABclonal), anti-GAPDH antibody (1:5000; Sigma-Aldrich, Saint Louis, MO, USA) and anti-α-tubulin antibody (1:5000; Sigma-Aldrich). Immunoreactive bands were visualized by the ECL imaging system (GE Healthcare, Buckinghamshire, UK). Total intensities were semi-quantified using Quantity One software (Bio-Rad, Hercules, CA, USA).

For lectin immunoprecipitation, cell lysate (1 mg) or HCC tissue lysate (500 μg) were incubated with 40 μL SNA- or MAL-agarose beads (Vector Laboratories) for 1 h at 4 °C. For co-immunoprecipitation assay, cell lysate (1 mg) was incubated with anti-MCAM antibody (CST) overnight at 4 °C

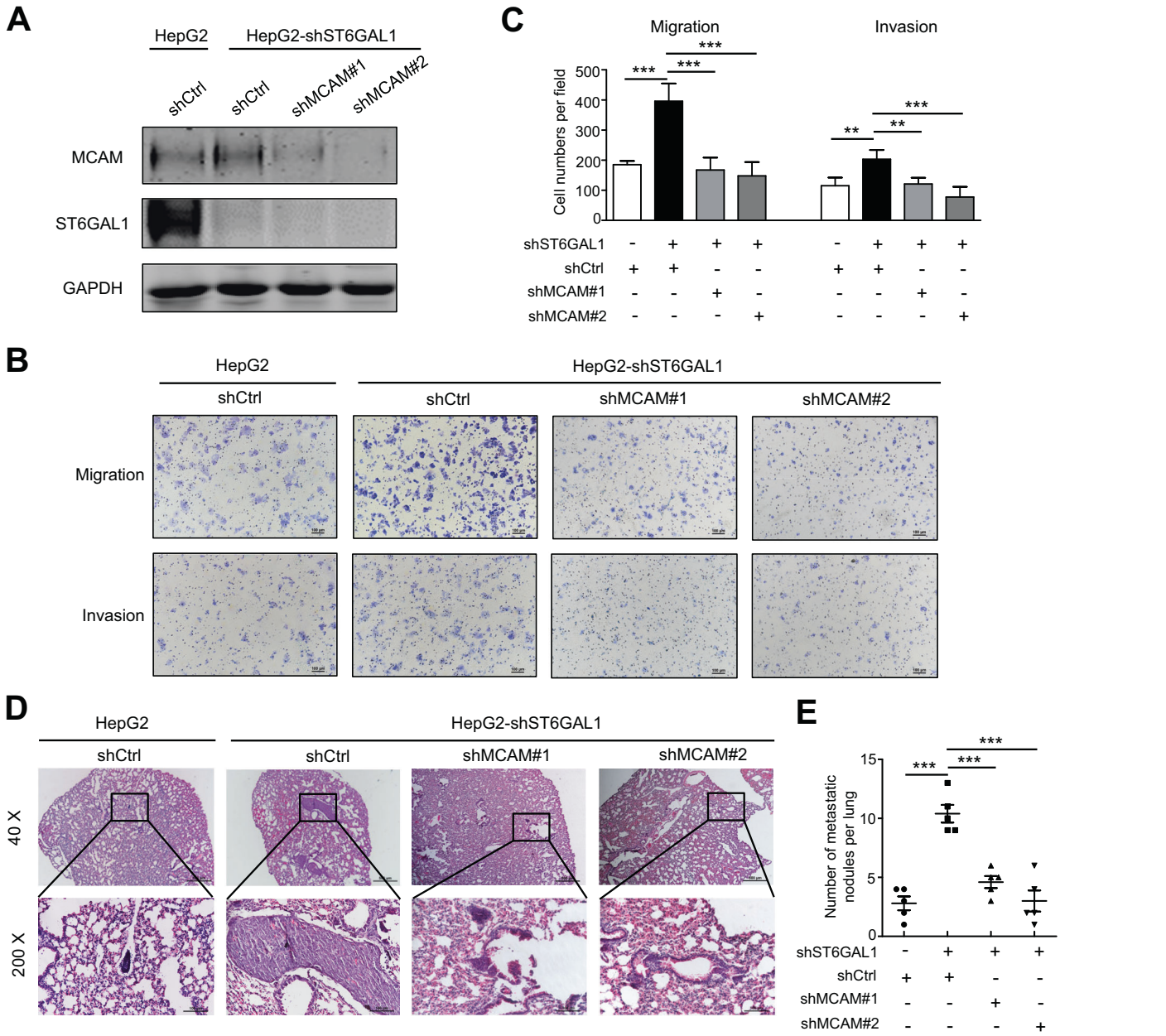

Fig. 6 ST6GAL1 loss promotes HCC metastasis by up-regulating MCAM. HepG2 and ST6GAL1-deficient HepG2 cells were stably transfected with shCtrl or shMCAM (shMCAM#1 and shMCAM#2) plasmids to generate control (shCtrl), ST6GAL1-knockdown (shST6GAL1 + shCtrl), as well as ST6GAL1-knockdown and MCAM-knockdown (shST6GAL1 + shMCAM#1 and shST6GAL1 + shMCAM#2) stable cells. **A** Western blot analysis confirmed MCAM and ST6GAL1 knockdown in HepG2 cells. **B** Transwell analysis showed that MCAM knockdown reduced the promoted migration and invasion in ST6GAL1 silencing cells. **C** Statistic analysis of the number of migratory and invasive cells in Fig. 6B. Data were shown as mean ± SD of three independent experiments. **D** H&E staining of lung tissue sections showed that MCAM knockdown abolished the increased incidence and volume of lung metastases of HCC in ST6GAL1 silencing cells. The above indicated cells (2×10^6) were injected into the tail vein of 5- to 6-weeks old male BALB/c nude mice ($n = 5$ for each group). After eight weeks, the lungs were collected and the number of lung metastatic foci in each group was calculated. Data were shown as mean ± SEM. Statistical analysis was performed using unpaired two-tailed Student's *t* tests. $^{**}p < 0.01$; $^{***}p < 0.001$.

with gentle rotation. The MCAM-bound proteins were immunoprecipitated for 3 h at 4 °C using Protein G-agarose beads (Roche, Indianapolis, IN, USA). After washing three times with lysis buffer or TBS, the immunoprecipitates were eluted with 30 µL TBS containing 0.2% SDS at 95 °C for 10 min and subjected to 7.5% SDS-PAGE.

Quantitative real-time PCR (qRT-PCR)

Total RNA was prepared with TRI reagent (Invitrogen, Carlsbad, CA, USA), and 1 µg total RNA was reverse-transcribed to 20 µL cDNA using a PrimeScript RT reagent Kit with gDNA Eraser (Takara, Shiga, Japan). The primer sequences for qRT-PCR were as follows: ST6GAL1 (5′-AAAAACCTTATCCCTAGGCTGC-3′ and 5′-TGGTAGTTTTTGTGCCCACA-3′), MCAM (5′-AAACATCCAGGTCAACCCCC-3′ and 5′-ACCACTCGACTCCACAGTCT-3′), and GAPDH (5′-ATGTTCGTCATGGGTGTGAA-3′ and 5′-GTCTTCTGGGTGGCAGTGAT-3′). GAPDH was used as an internal control.

Cell migration and invasion assays

Cell migration and invasion were examined using Transwell chambers (8.0-µm inserts; Corning, Tewksbury, MA, USA) in 24-well plate. For migration assays, HCC cells were starved in serum-free medium for 12 h. Then,

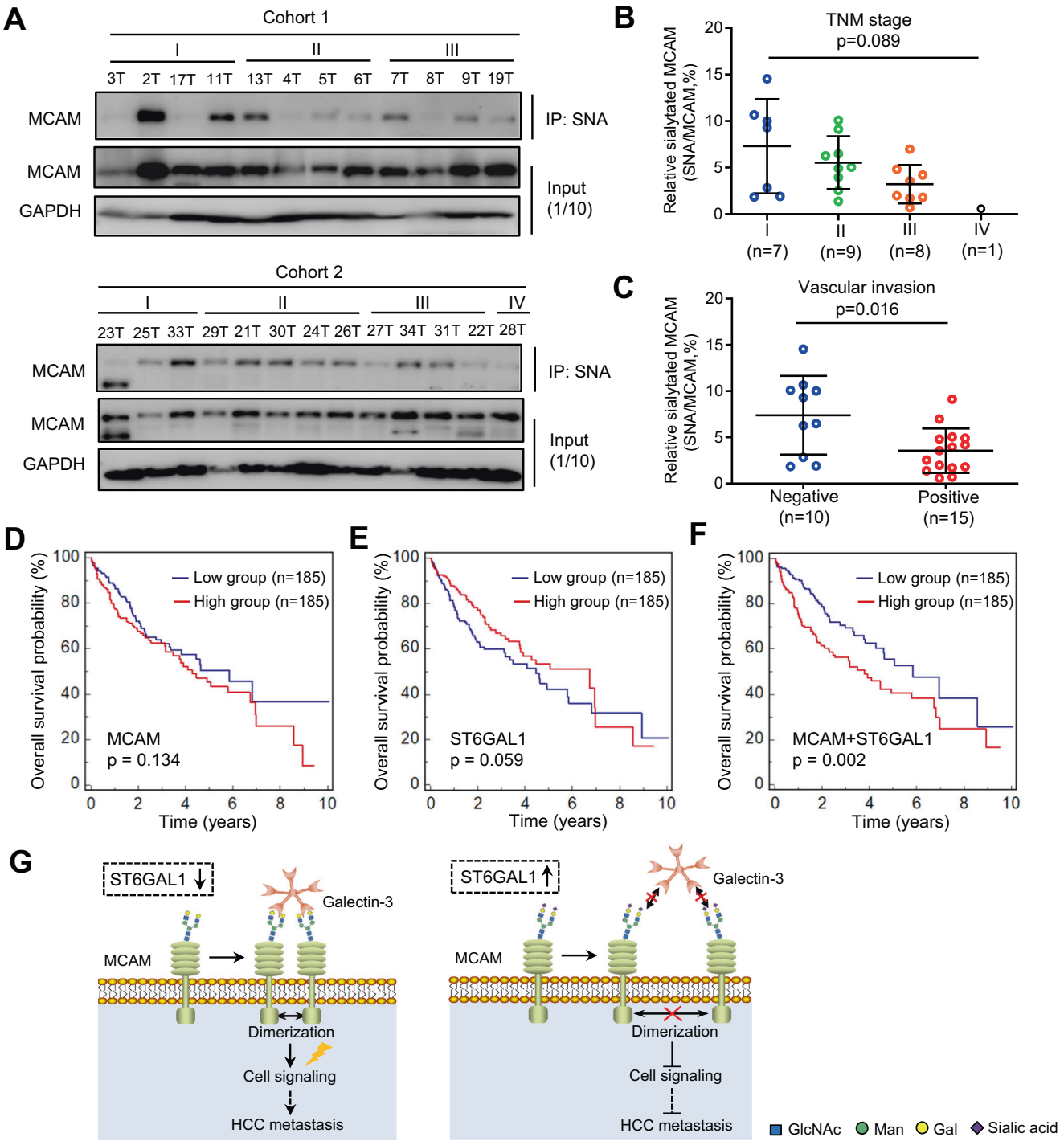

Fig. 7 Expression and prognostic value of sialylated MCAM in human HCC tissues. A Lectin immunoprecipitation analysis showing the expression level of sialylated MCAM in human HCC tumor tissues. Tissue lysate from two clinic cohorts ($n = 25$) were immunoprecipitated by SNA-agarose beads and immunoblotted with anti-MCAM antibody (top, sialylated MCAM). The total MCAM of tissue lysate before SNA enrichment were detected in input samples (middle). The ratio of sialylated MCAM to total MCAM was considered as the relative intensity of sialylated MCAM in each sample. The relative intensities of sialylated MCAM were negatively associated with TNM stage (**B**) and vascular invasion (**C**) in HCC patients. Statistical analysis was performed using two-tailed Kruskal-Wallis test (**B**) and unpaired two-tailed Student's *t* tests (**C**). Prognostic value of MCAM (**D**), ST6GAL1 (**E**) and the combination of MCAM and ST6GAL1 (**F**) using binary logistic regression model ($y = 0.197*MCAM-0.168*ST6GAL1–0.210$) were analyzed by Kaplan-Meier analysis of overall survival in 370 HCC samples from TCGA database. The cutoff values were the median values. Log-rank test was used to compare survival of patients between subgroups. **G** A possible mechanism underlying how ST6GAL1 regulates MCAM dimerization through galectin 3 interaction during HCC metastasis. SNA *Sambucus nigra* agglutinin, T tumor, GlcNAc N-acetylglucosamine, Man mannose, Gal galactose.

MHCC97L (2×10^5) cells, HCCLM3 (2×10^5) cells and HepG2 (3×10^5) cells were suspended in 500 µL serum-free medium and seeded into the upper chambers. The lower chambers were filed with 800 µL culture medium containing 10% FBS. After incubation at 37 °C for 48 h, the cells remaining on the upper membrane were carefully wiped off with cotton swab, while the cells that had invaded through the membranes were fixed with 4% paraformaldehyde for 30 min at room temperature and stained with 0.5% crystal violet at 37 °C for 1 h. For the invasion assays, transwell chambers were precoated with Matrigel (BD Biosciences) and other steps were the same with that in migration assays.

Flow cytometry

Cells were grown to approximately 90% confluence, detached using trypsin containing 1 mM EDTA at 37 °C, and washed three times with cold PBS. To analyze the sialic acid on cell surface, cells were stained with 10 µg/mL biotinylated SNA or MAL (Vector Laboratories) for 30 min on ice, followed by incubation with Alexa Fluor 488-conjugated streptavidin (Invitrogen) for 30 min on ice. To analyze MCAM expression on cell surface, cells were stained with anti-MCAM antibody (1:100, Proteintech, Wuhan, China) for 1 h at 4 °C, followed by incubation with streptavidin- Alexa Fluor 488-conjugated goat anti-rabbit IgG (1:500, Thermo Fisher Scientific, Waltham, MA, USA) for 1 h on ice. Finally, cells were washed three times with PBS and analyzed by flow cytometry (BD Biosciences).

Immunofluorescence staining

Cells were seeded onto glass coverslips in 12-well plate (1.5×10^5/well) and cultured in 10% FBS/DMEM at 37 °C overnight. After treating with either recombinant galectin-3 (2 µg/mL) or BSA (2 µg/mL) for 1 h, the cells were washed with ice-cold PBS and fixed with 4% paraformaldehyde for 10 min at 4 °C. The cells were blocked in 5% BSA/PBS (w/v) for 2 h at room temperature, followed by incubated with anti-galectin-3 (1:100; Proteintech) or anti-MCAM (1:100; Abways, Shanghai, China) at 4 °C overnight. After three washes with PBS, the cells were incubated with Alexa Fluor 594- (1:400; Invitrogen) or 647- (1:400; Invitrogen) conjugated secondary antibodies or FITC-conjugated SNA (1:200; EY Laboratories, San Mateo, CA, USA) for 1 h at room temperature. DAPI was used to stain the nucleus. The slides were visualized on a Nikon A1Si laser-scanning confocal microscope.

Lectin microarray analysis

Lectin microarray analysis was performed as described previously with some modification [50]. Briefly, membrane proteins from cells (2×10^6) were extracted using a CelLytic MEM Protein Extraction Kit (Sigma-Aldrich). The fractions were fluorescently labeled with 10 µg of Cy3-succinimidyl ester (GE Healthcare) for 1 h at room temperature in the dark. The sample solution was diluted with probing buffer (500 mM glycine, 1 mM $CaCl_2$, and 1 mM $MnCl_2$ in Tris-buffered saline containing 1% Triton X-100) and incubated at room temperature for 2 h to block excess fluorescent reagent. An appropriate aliquot of Cy3-labeled glycoprotein was applied to one well on a lectin microarray chip (LecChip™ Ver. 1.0, GlycoTechnica, Yokohama, Japan) containing 45 lectins (Supplementary Table S1) and incubated overnight at 20 °C. Fluorescence signals were measured using a GlycoStation™ Reader 1200 (GlycoTechnica). Data were calculated using image analyzer software (GlycoStation™ ToolsPro Suite ver. 1.5, GlyoTechnica) and normalized using the mean-normalization method.

Metabolic labeling

Metabolic labeling was performed as described previously [48]. Cells (4×10^6) were treated with 100 µM Ac_4ManNAz or ManNAc for 60 h. After metabolic labeling, the cells were lysed and incubated with biotinylated alkyne and 1 µL catalytic solution of 200 mM CuSO4, 20 mM TBTA, 400 mM sodium ascorbate (freshly prepared and mixed). The mixture was vortexed at 1400 rpm for 1 h at room temperature to complete the click reaction. The labeling efficiency was assessed by immunoblotting with streptavidin-680 (Invitrogen).

Mass spectrometry (MS)

After washing with PBS, 1×10^7 metabolically labeled cells were subjected to the click reaction with biotinylated alkyne and glycoproteins were enriched by streptavidin-agarose resin. The proteins were reduced and alkylated followed by on-bead trypsin digestion. The released peptides were analyzed on a Q Exactive Plus mass spectrometer equipped with an Easy-nLC 1000 (Thermo Fisher Scientific). Spectra were searched against a human proteins database using the Andromeda module of MaxQuant software v. 1.5.5.1 as described previously [48]. The relative iBAQ value was used to represent the normalized abundance of a particular protein across samples.

Bioinformatic annotation and analysis

Membrane proteins were predicted using TMHMM-2.0 server (https://services.healthtech.dtu.dk/service.php?TMHMM-2.0). Gene ontology (GO) enrichment analysis was carried out using DAVID Bioinformatics Resources 6.8 (https://david.ncifcrf.gov/). Functional analysis was conducted using Ingenuity Pathways Analysis (IPA) software v7.1 (Ingenuity Systems, Mountain View, CA).

Statistical analysis

Statistical calculations were conducted with SPSS version 16.0 and GraphPad Prism 5. To compare two groups, Student's *t*-test or the Mann–Whitney *U*-test was implemented. In cases of more than two groups, one-way analysis of variance (parametric test) or the Kruskal–Wallis test (non parametric test) was used. Survival was calculated by Kaplan-Meier analysis (log-rank test) using MedCalc version 15.0. A p value of less than 0.05 was considered statistically significant.

DATA AVAILABILITY

The datasets generated and/or analysed during the current study are available from the corresponding author on reasonable request.

REFERENCES

1. Sung H, Ferlay J, Siegel RL, Laversanne M, Soerjomataram I, Jemal A, et al. Global cancer statistics 2020: GLOBOCAN estimates of incidence and mortality worldwide for 36 cancers in 185 countries. CA Cancer J Clin. 2021;71:209–49.
2. Chen W, Zheng R, Baade PD, Zhang S, Zeng H, Bray F, et al. Cancer statistics in China, 2015. CA Cancer J Clin. 2016;66:115–32.
3. Siegel RL, Miller KD, Jemal A. Cancer statistics, 2020. CA Cancer J Clin. 2020;70:7–30.
4. Wu C, Ren X, Zhang Q. Incidence, risk factors, and prognosis in patients with primary hepatocellular carcinoma and lung metastasis: a population-based study. Cancer Manag Res. 2019;11:2759–68.
5. Varki A. Biological roles of glycans. Glycobiology. 2017;27:3–49.
6. Pinho SS, Reis CA. Glycosylation in cancer: mechanisms and clinical implications. Nat Rev Cancer. 2015;15:540–55.
7. Mereiter S, Balmana M, Campos D, Gomes J, Reis CA. Glycosylation in the era of cancer-targeted therapy: where are we heading? Cancer Cell. 2019;36:6–16.
8. Silsirivanit A. Glycosylation markers in cancer. Adv Clin Chem. 2019;89:189–213.
9. Lu J, Gu J. Significance of beta-galactoside alpha2,6 sialyltranferase 1 in cancers. Molecules. 2015;20:7509–27.
10. Garnham R, Scott E, Livermore KE, Munkley J. ST6GAL1: a key player in cancer. Oncol Lett. 2019;18:983–9.
11. Britain CM, Bhalerao N, Silva AD, Chakraborty A, Buchsbaum DJ, Crowley MR, et al. Glycosyltransferase ST6Gal-I promotes the epithelial to mesenchymal transition in pancreatic cancer cells. J Biol Chem. 2021;296:100034.
12. Wichert B, Milde-Langosch K, Galatenko V, Schmalfeldt B, Oliveira-Ferrer L. Prognostic role of the sialyltransferase ST6GAL1 in ovarian cancer. Glycobiology 2018;28:898–903.
13. Lu J, Isaji T, Im S, Fukuda T, Hashii N, Takakura D, et al. beta-Galactoside alpha2,6-sialyltranferase 1 promotes transforming growth factor-beta-mediated epithelial-mesenchymal transition. J Biol Chem. 2014;289:34627–41.
14. Wang PH, Li YF, Juang CM, Lee YR, Chao HT, Ng HT, et al. Expression of sialyltransferase family members in cervix squamous cell carcinoma correlates with lymph node metastasis. Gynecol Oncol. 2002;86:45–52.
15. Gessner P, Riedl S, Quentmaier A, Kemmner W. Enhanced activity of CMP-neuAc:Gal beta 1-4GlcNAc:alpha 2,6-sialyltransferase in metastasizing human colorectal tumor tissue and serum of tumor patients. Cancer Lett. 1993;75:143–9.
16. Gretschel S, Haensch W, Schlag PM, Kemmner W. Clinical relevance of sialyltransferases ST6GAL-I and ST3GAL-III in gastric cancer. Oncology 2003;65:139–45.
17. Christie DR, Shaikh FM, Lucas JAT, Lucas JA 3rd, Bellis SL. ST6Gal-I expression in ovarian cancer cells promotes an invasive phenotype by altering integrin glycosylation and function. J Ovarian Res. 2008;1:3.
18. Holdbrooks AT, Britain CM, Bellis SL. ST6Gal-I sialyltransferase promotes tumor necrosis factor (TNF)-mediated cancer cell survival via sialylation of the TNF receptor 1 (TNFR1) death receptor. J Biol Chem. 2018;293:1610–22.

19. Tang ZY, Ye SL, Liu YK, Qin LX, Sun HC, Ye QH, et al. A decade's studies on metastasis of hepatocellular carcinoma. J Cancer Res Clin Oncol. 2004;130:187–96.
20. Jiang G, Zhang L, Zhu Q, Bai D, Zhang C, Wang X. CD146 promotes metastasis and predicts poor prognosis of hepatocellular carcinoma. J Exp Clin Cancer Res. 2016;35:38.
21. Wang J, Tang X, Weng W, Qiao Y, Lin J, Liu W, et al. The membrane protein melanoma cell adhesion molecule (MCAM) is a novel tumor marker that stimulates tumorigenesis in hepatocellular carcinoma. Oncogene. 2015;34:5781–95.
22. Stalin J, Nollet M, Garigue P, Fernandez S, Vivancos L, Essaadi A, et al. Targeting soluble CD146 with a neutralizing antibody inhibits vascularization, growth and survival of CD146-positive tumors. Oncogene. 2016;35:5489–500.
23. Zhang Z, Zheng Y, Wang H, Zhou Y, Tai G. CD146 interacts with galectin-3 to mediate endothelial cell migration. FEBS Lett. 2018;592:1817–28.
24. Colomb F, Wang W, Simpson D, Zafar M, Beynon R, Rhodes JM, et al. Galectin-3 interacts with the cell-surface glycoprotein CD146 (MCAM, MUC18) and induces secretion of metastasis-promoting cytokines from vascular endothelial cells. J Biol Chem. 2017;292:8381–9.
25. Zhuo Y, Bellis SL. Emerging role of alpha2,6-sialic acid as a negative regulator of galectin binding and function. J Biol Chem. 2011;286:5935–41.
26. Hirabayashi J, Hashidate T, Arata Y, Nishi N, Nakamura T, Hirashima M, et al. Oligosaccharide specificity of galectins: a search by frontal affinity chromatography. Biochim Biophys Acta. 2002;1572:232–54.
27. Dobie C, Skropeta D. Insights into the role of sialylation in cancer progression and metastasis. Br J Cancer. 2021;124:76–90.
28. Poon TC, Chiu CH, Lai PB, Mok TS, Zee B, Chan AT, et al. Correlation and prognostic significance of beta-galactoside alpha-2,6-sialyltransferase and serum monosialylated alpha-fetoprotein in hepatocellular carcinoma. World J Gastroenterol. 2005;11:6701–6.
29. Dall'Olio F, Chiricolo M, D'Errico A, Gruppioni E, Altimari A, Fiorentino M, et al. Expression of beta-galactoside alpha2,6 sialyltransferase and of alpha2,6-sialylated glycoconjugates in normal human liver, hepatocarcinoma, and cirrhosis. Glycobiology. 2004;14:39–49.
30. Antony P, Rose M, Heidenreich A, Knuchel R, Gaisa NT, Dahl E. Epigenetic inactivation of ST6GAL1 in human bladder cancer. BMC Cancer. 2014;14:901.
31. Yamamoto H, Kaneko Y, Rebbaa A, Bremer EG, Moskal JR. alpha2,6-Sialyltransferase gene transfection into a human glioma cell line (U373 MG) results in decreased invasivity. J Neurochem. 1997;68:2566–76.
32. Yamamoto H, Oviedo A, Sweeley C, Saito T, Moskal JR. Alpha2,6-sialylation of cell-surface N-glycans inhibits glioma formation in vivo. Cancer Res. 2001;61:6822–9.
33. Zhu Y, Srivatana U, Ullah A, Gagneja H, Berenson CS, Lance P. Suppression of a sialyltransferase by antisense DNA reduces invasiveness of human colon cancer cells in vitro. Biochim Biophys Acta. 2001;1536:148–60.
34. Seales EC, Jurado GA, Brunson BA, Wakefield JK, Frost AR, Bellis SL. Hypersialylation of beta1 integrins, observed in colon adenocarcinoma, may contribute to cancer progression by up-regulating cell motility. Cancer Res. 2005;65:4645–52.
35. Petretti T, Kemmner W, Schulze B, Schlag PM. Altered mRNA expression of glycosyltransferases in human colorectal carcinomas and liver metastases. Gut. 2000;46:359–66.
36. Jung YR, Park JJ, Jin YB, Cao YJ, Park MJ, Kim EJ, et al. Silencing of ST6Gal I enhances colorectal cancer metastasis by down-regulating KAI1 via exosome-mediated exportation and thereby rescues integrin signaling. Carcinogenesis. 2016;37:1089–97.
37. Zhou L, Zhang S, Zou X, Lu J, Yang X, Xu Z, et al. The beta-galactoside alpha2,6-sialyltranferase 1 (ST6GAL1) inhibits the colorectal cancer metastasis by stabilizing intercellular adhesion molecule-1 via sialylation. Cancer Manag Res. 2019;11:6185–99.
38. Oswald DM, Zhou JY, Jones MB, Cobb BA. Disruption of hepatocyte Sialylation drives a T cell-dependent pro-inflammatory immune tone. Glycoconj J. 2020;37:395–407.
39. Dorsett KA, Marciel MP, Hwang J, Ankenbauer KE, Bhalerao N, Bellis SL. Regulation of ST6GAL1 sialyltransferase expression in cancer cells. Glycobiology 2021;31:530–9.
40. Kroes RA, Moskal JR. The role of DNA methylation in ST6Gal1 expression in gliomas. Glycobiology. 2016;26:1271–83.
41. Huang G, Li Z, Li Y, Liu G, Sun S, Gu J, et al. Loss of core fucosylation in both ST6GAL1 and its substrate enhances glycoprotein sialylation in mice. Biochem J. 2020;477:1179–201.
42. Zhou Y, Fukuda T, Hang Q, Hou S, Isaji T, Kameyama A, et al. Inhibition of fucosylation by 2-fluorofucose suppresses human liver cancer HepG2 cell proliferation and migration as well as tumor formation. Sci Rep. 2017;7:11563.
43. Shan M, Yang D, Dou H, Zhang L. Fucosylation in cancer biology and its clinical applications. Prog Mol Biol Transl Sci. 2019;162:93–119.
44. Swindall AF, Bellis SL. Sialylation of the Fas death receptor by ST6Gal-I provides protection against Fas-mediated apoptosis in colon carcinoma cells. J Biol Chem. 2011;286:22982–90.
45. Wang Z, Xu Q, Zhang N, Du X, Xu G, Yan X. CD146, from a melanoma cell adhesion molecule to a signaling receptor. Signal Transduct Target Ther. 2020;5:148.
46. Bu P, Zhuang J, Feng J, Yang D, Shen X, Yan X. Visualization of CD146 dimerization and its regulation in living cells. Biochim Biophys Acta. 2007;1773:513–20.
47. Croci DO, Cerliani JP, Dalotto-Moreno T, Mendez-Huergo SP, Mascanfroni ID, Dergan-Dylon S, et al. Glycosylation-dependent lectin-receptor interactions preserve angiogenesis in anti-VEGF refractory tumors. Cell. 2014;156:744–58.
48. Zhang S, Lu J, Xu Z, Zou X, Sun X, Xu Y, et al. Differential expression of ST6GAL1 in the tumor progression of colorectal cancer. Biochem Biophys Res Commun. 2017;486:1090–6.
49. Yi CH, Weng HL, Zhou FG, Fang M, Ji J, Cheng C, et al. Elevated core-fucosylated IgG is a new marker for hepatitis B virus-related hepatocellular carcinoma. Oncoimmunology. 2015;4:e1011503.
50. Zou X, Yoshida M, Nagai-Okatani C, Iwaki J, Matsuda A, Tan B, et al. A standardized method for lectin microarray-based tissue glycome mapping. Sci Rep. 2017;7:43560.

ACKNOWLEDGEMENTS

We thank Dr. Yanmin Yu (Ruijin Hosptial, Shanghai Jiao Tong University School of Medicine) for her help in the pathological interpretation of tissue arrays.

AUTHOR CONTRIBUTIONS

Conception and design: YZ, JL; Development of methodology: XZ, JL, XY, YC; Acquisition of data: XZ, JL, YD, QL, XY, YC, XX, MF, FY, HS, BT, XL; Analysis and interpretation of data: XZ, JL, YD, YZ; Technical or material support: CG, HN, AK, TS, BF; Writing—original draft: XZ, JL; Writing—review and editing: YZ, CG, HN, AK, TS; Study supervision: YZ.

FUNDING

This work was supported by the by the National Science and Technology Major Project of China (2018ZX10302-205-003-002), the National Natural Science Foundation of China (32071271, 31770850, 31600643 and 81802100), the Innovation Group Project of Shanghai Municipal Health Commission (2019CXJQ03).

COMPETING INTERESTS

The authors declare no competing interests.

ADDITIONAL INFORMATION

Supplementary information The online version contains supplementary material available at https://doi.org/10.1038/s41388-022-02571-9.

Correspondence and requests for materials should be addressed to Yan Zhang.

Reprints and permission information is available at http://www.nature.com/reprints

Publisher's note Springer Nature remains neutral with regard to jurisdictional claims in published maps and institutional affiliations.